Major effects of sensory experiences on the neocortical inhibitory circuits

Yuanyuan Jiao[1,2,] Chunzhao Zhang[1], Yuchio Yanagawa[3] and Qian-Quan Sun[1,2 *]

1. Department of Zoology and Physiology, University of Wyoming, Laramie, WY 82071. 2. Neuroscience Program, University of Wyoming, Laramie, WY 82071. 3. Department of Genetic and Behavioral Neuroscience, Gunma University Graduate School of Medicine and SORST, JST, Maebashi 371-8511, Japan. * author of Correspondence: neuron@uwyo.edu

717

1. Summary

This project seeks to understand how the structure and organization of the brain adapt to changes in sensory information. The scientific objective was to identify how different types of sensory stimulation affect the organization, development, and function of neural systems. We have found that early sensory experiences have profound effects on the fine structural and functional organization of the mature brain circuits. Sensory deprivation (such as child neglect) can induce long-term changes in the way the brain is organized and how neurons, the cells of the brain, are interconnected and function.

2. Methods

2.1. Immunohistological studies

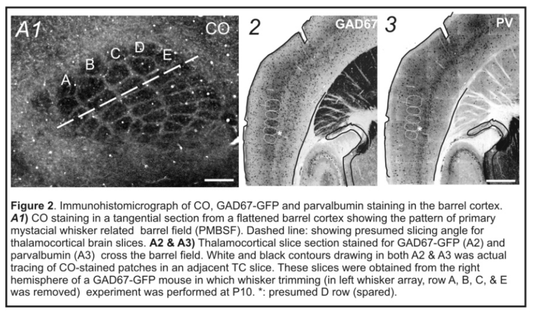

Figure 2. Immunohistomicrograph of CO, GAD67-GFP and parvalbumin staining in the barrel cortex. ***A1)*** CO staining in a tangential section from a flattened barrel cortex showing the pattern of primary mystacial whisker related barrel field (PMBSF). Dashed line: showing presumed slicing angle for thalamocortical brain slices. **A2 & A3)** Thalamocortical slice section stained for GAD67-GFP (A2) and parvalbumin (A3) cross the barrel field. White and black contours drawing in both A2 & A3 was actual tracing of CO-stained patches in an adjacent TC slice. These slices were obtained from the right hemisphere of a GAD67-GFP mouse in which whisker trimming (in left whisker array, row A, B, C, & E was removed) experiment was performed at P10. *: presumed D row (spared).

2.2.Patch-clamp recordings in GFP mouse

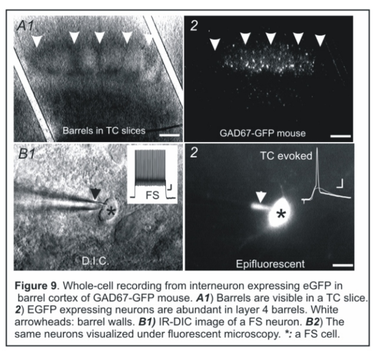

Figure 9. Whole-cell recording from interneuron expressing eGFP in barrel cortex of GAD67-GFP mouse. ***A1)*** Barrels are visible in a TC slice. **2**) EGFP expressing neurons are abundant in layer 4 barrels. White arrowheads: barrel walls. ***B1)*** IR-DIC image of a FS neuron. ***B2***) The same neurons visualized under fluorescent microscopy. *: a FS cell.

3.1 W.T. Primarily affects PV-positive interneurons in the barrel cortex layer IV.

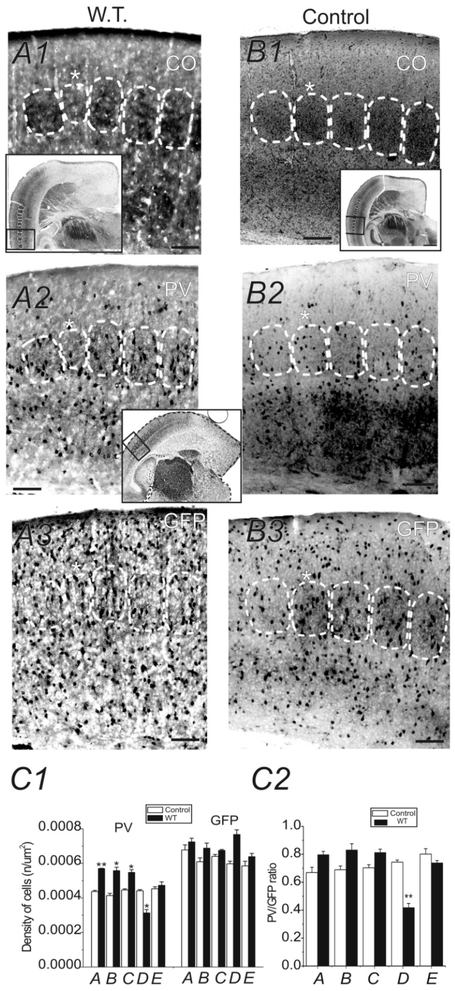

Figure 1. Effects of row-D WT on PV expression in barrel cortex layer 4 (TC sections). A1& B1) Photomicrograph of a CO stained TC section (40 μm in thickness) from a row D whisker trimmed GAD67-GFP mouse (A1) and a control liter mate mouse (B1). White dashed lines outlined barrels throughout layer IV of the barrel cortex. Asterisk marked row D of barrel field. Note the reduction in barrel size of row D. Scale bar=150 m (for A1-3 and B1-3). Insets in A1 & B1: image of entire TC sections. The box in insets showed areas of PMBSF (posteromedial barrel subfield) that were enlarged and shown in A1 & B1. Scale bar in B1 inset=600 m. A2&3) Two adjacent brain sections (40 μm in thickness) to the CO-stained section of A1. The sections were stained for PV (A2) and GFP (A3), respectively. Rows A-E barrel areas of layer IV barrel cortex were shown. B2&3) two brain sections adjacent to the section of B1. The sections were stained for PV (B2) and GFP (B3), respectively. C1) Statistical comparison of cell densities (PV-positive and GFP-positive cells, respectively) in row A-E barrels of WT (black bars) and normal mice (white bars). Only neurons inside the barrels were counted. C2) Comparison of PV/GFP ratio in row A-E barrels of WT (black bars) and normal mice (white bars). *: p<0.05; **: p<0.01; n=5 brains in WT and controls, respectively.

3. Results

3.2 W.T. Induced robust down-regulation of PV in interneurons of layer IV

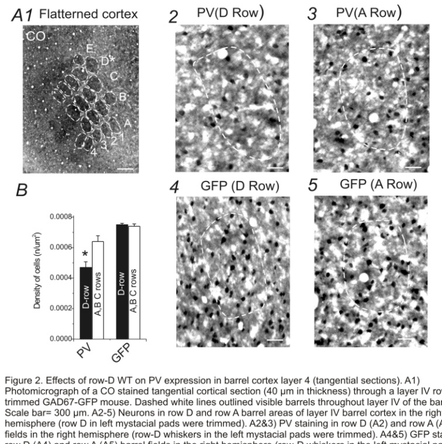

Figure 2. Effects of row-D WT on PV expression in barrel cortex layer 4 (tangential sections). A1) Photomicrograph of a CO stained tangential cortical section (40 μm in thickness) through a layer IV row D trimmed GAD67-GFP mouse. Dashed white lines outlined visible barrels throughout layer IV of the barrel cortex. Scale bar= 300 μm. A2-5) Neurons in row D and row A barrel areas of layer IV barrel cortex in the right hemisphere (row D in left mystacial pads were trimmed). A2&3) PV staining in row D (A2) and row A (A3) barrel fields in the right hemisphere (row-D whiskers in the left mystacial pads were trimmed). A4&5) GFP staining in row D (A4) and row A (A5) barrel fields in the right hemisphere (row-D whiskers in the left mystacial pads were trimmed). Only neurons inside the barrels were counted. Scale bar= 50μm. B) Density of PV-positive and GFP-positive neurons in row D barrels (black bars) and spared barrels (rows A-C, white bars).

3.3 W.T. induces robust down-regulation of perisomatic inhibitory synaspes in spiny cells

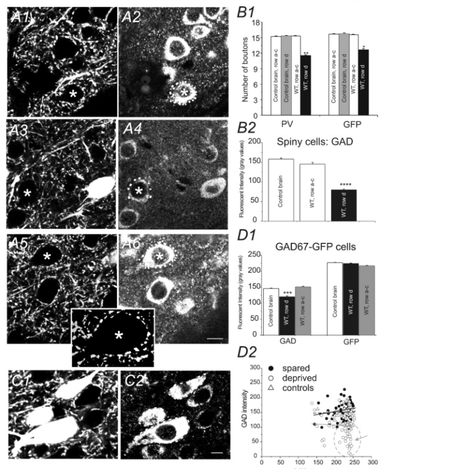

Figure 4. Photomicrograph of GFP (A1, A3,& A5) and GAD65&67-IR (A2, A4 & A6) in layer IV barrel cortex. A1& A2: control untreated mouse. A3 & A4: deprived row (D). A5 & A6: spared row. Scale bars=10 m. Dotted (white) lines in A2, A4 & A6 demarcate a GFP-negative area (*) innervated by GFP-positive boutons in A1, A2 & A3, respectively. Inset in A5: digitally enhanced micrograph of the perisomatic GFP puncta marked by an asterisk in A5. B1) Number of PV-positive and GFP-positive perisomatic varicosities near a presumed spiny neuron in barrels of tangential slices from control mice (white bars) and WT (row D trimmed) mice (black bars), respectively. B2) Fluorescent intensities for GAD65& 67-IR in presumed spiny neurons demarked by the GFP-positive presynaptic varicosities (e.g. A2, A4 &A6) in TC slices from control mice (white bar), deprived region (row D, black bar) and spared region (row A-C, gray bar) of WT treated mice, respectively. C) Photomicrograph of GFP (C1) and GAD65&67-IR (C2) in layer IV barrel cortex of a naive untreated GAD67-GFP mouse. D1) Bar graph show changes in expression of GAD65& 67-IR and GFP in the GFP cells located in barrels of control, deprived and spared cortices. D2) Scatter plots showed relationship between expression of GFP and GAD65&67-IR in barrels of control mice (open triangles), WT treated mice [spared (filled black circles) and deprived (open circles) sites, respectively).

3.4 Effects of WT on inhibitory synaptic transmission in barrel cortex layer IV

Table 1. Comparison of properties of mIPSCs from spiny neurons in spared and deprived barrels of treated mice and controls (P30 and P7)

Location	Amplitude (pA)	Half width (ms)	τ_{decay} (ms)	C.V.	Instant Frequency	R_{in} (MΩ)	N.
Spared	17 ±0.2	35±0.5	16±1.0	0.4±0.1	15±5	245±31	22
Deprived	11 ±0.2**	38 ±0.6*	17±0.2*	0.5±0.1*	6±0.6**	217±37**	20
Controls (P30)	16±0.3	36±1	16±1.0	0.4±0.1	14±2	252±27	35
Controls (P7)	24±5*	43±1.9*	30±3**	0.5±0.1*	3±1.4**	221±41*	15

C.V.: Coefficient of variation for mIPSC amplitude; R_{in}*: Input resistance.***: p<0.01; *: p<0.05, deprived vs. spared and P7 vs. P30 controls.*

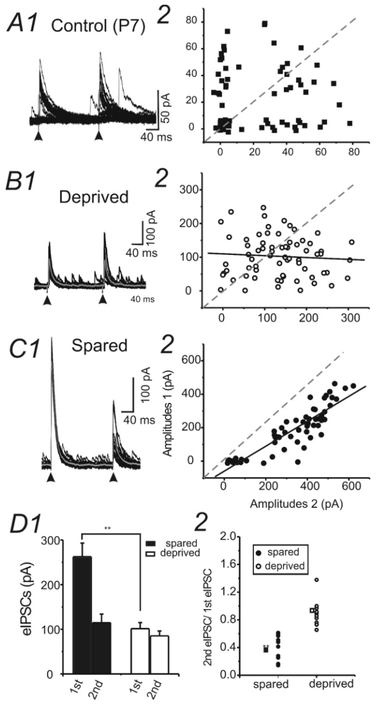

Figure 7. Properties of eIPSCs recorded in spiny neurons in control (P7 & P30) and WT treated brain slices. A1) Example of eIPSCs evoked by extracellular stimuli at an interval of 200 ms in a cell in barrel cortex layer IV of P7 mouse. Vhold=0 mV. A2) Amplitudes of eIPSC1 were plotted against the amplitudes of eIPSC2 in the same cell. Dashed line: level at which amplitudes of eIPSC1 equal to amplitudes of eIPSC2. B1 & C1) Example of eIPSCs evoked by extracellular stimuli at an interval of 200 ms in cells located in 'spared regions' (C1) and in 'deprived region' (B1) in barrel cortex layer IV, respectively. Vhold=0 mV. Thicker gray traces: averaged trace for recordings of A1 & B1. B2 & C2) Amplitudes of eIPSC1 were plotted against the amplitudes of eIPSC2 in the same cell. Solid black line: linear fitting for the scatter plot. Dashed line: level at which amplitudes of EPSC1 equal to amplitudes of EPSC2. Note that in cell of C1, amplitudes 2 were always smaller than the amplitudes 1, therefore the data points were all located below the dashed line; however, in cell of B1, similar pattern of distribution did not exist. D1) The mean amplitudes of eIPSCs evoked by the extracellular stimuli in 'spared' and 'deprived' barrels. **: p<0.01, n=10 for each group. D2) The paired pulse ratio of eIPSCs in cells located in spared (filled circles) and deprived (open circles) barrels. **: p<0.01, n=10 for each group.

4. Conclusion

4.1. We showed specific structural and anatomical changes (i.e. the number of perisomatic inhibitory synapses) occurred in specific types (i.e. PV-positive) of interneurons and that these changes were associated with a lack of sensory experience during the second and the third postnatal week.

4.2. We have also found that the reduction of presynaptic perisomatic inhibitory boutons was found to exist concomitantly with functionally abnormal inhibitory synaptic transmission in spiny neurons.

4.3. These results suggest that postnatal sensory activities in vivo are necessary for the transformation of functional inhibitory transmission from an immature to a mature phenotype.

4.4. We suggest that whisker specific thalamocortical activities and down-stream local cortical activities, and not activities provided by surrounding whiskers, are important for the postnatal maturation of inhibitory networks.

4.5. Cortical disinhibition, as a consequence of selective whisker removal, is likely to be an important factor underlying altered receptive field property in sensory-deprived animals (cf. Kelly et al., 1999).

Funded by NIH-NCRR